

# Acid-Labile Polyvinylamine Micro- and Nanogel Capsules

Lianjun Shi<sup>‡</sup> and Cory Berkland<sup>\*,†,‡</sup>

Department of Pharmaceutical Chemistry and Department of Chemical and Petroleum Engineering,  
The University of Kansas, Lawrence, Kansas 66047

Received February 19, 2007; Revised Manuscript Received April 20, 2007

**ABSTRACT:** Hollow nanoparticles represent an emerging area of development for the encapsulation of active ingredients. Expanding the capabilities of these nanomaterials will require continued efforts to infill properties such as size control, biodegradability, and environmental responsiveness. Acid-labile poly(*N*-vinylformamide) (PNVF) nanocapsules were synthesized by free radical polymerization of *N*-vinylformamide on the surface of silica nanoparticles. Polymerization in the presence of a novel cross-linker that contains an acid-labile ketal facilitated stable etching of silica nanoparticle templates using sodium hydroxide and recovery of degradable PNVF nanocapsules. The formamide side group of PNVF was then hydrolyzed by extended exposure to sodium hydroxide to produce polyvinylamine (PVAm) micro- and nanocapsules. Both capsule types demonstrated an increasing dissolution rate as pH decreased. In addition, PVAm nanocapsules exhibited swelling in proportion to the relative charge density of the PVAm network (a function of the degree of formamide hydrolysis and pH), presumably due to the repulsion of positively charged amine groups within the elastic shell network. The synthetic approaches reported provide methods to endow nanocapsules with key attributes such as size control, pH sensitive degradation, swelling in response to pH, and amine functionality.

## Introduction

Hollow particles, also referred to as capsules or vesicles, are generating interest in industry as well as scientific research. Many active ingredients have been formulated within a capsule core to protect them from the surrounding environment and/or to facilitate sustained release including adhesives, agrochemicals, catalysts, living cells, flavor oils, pharmaceuticals, vitamins, etc.<sup>1–4</sup> Additional application areas continue to emerge. For example, hollow capsules have also received recent attention as mesoscopic reaction vessels.<sup>5</sup> These types of capsules may be attained by coating a core material or by forming hollow capsules *a priori* and then infilling the active ingredient. In many cases, forming hollow capsules *a priori* may be preferred. For example, the conditions necessary for the formation of a coating or shell may damage the active ingredient or the core material may confound shell formation. Expanding industrial implementation of capsules will require enhanced control of these materials at the nanoscale, development of capsules that are environmentally responsive, and/or synthesis of materials that are biodegradable, thus reducing their potential environmental or biological toxicity.

Several methods have been employed to fabricate polymer-based micro- and nanocapsules including self-assembly of amphiphilic block copolymers,<sup>6–8</sup> layer-by-layer (LbL) coating,<sup>9–11</sup> and interfacial or surface polymerization.<sup>12–14</sup> Bates et al. have demonstrated the utility of block copolymers self-assembled into “polymersomes”, which may be cross-linked within the hydrophobic region of the shell to improve the physical stability of these capsules.<sup>15,16</sup> In comparison to liposomes, polymersomes have demonstrated robust stability, acceptable drug loading, and controlled release.<sup>17,18</sup> The processes to fabricate hollow capsules by LbL and polymerization methods typically rely on the deposition of polymer films onto the surface of core templates

such as colloidal silica, CaCO<sub>3</sub>, etc., followed by the removal of the templates by appropriate chemical etching.<sup>19</sup> In the LbL method, oppositely charged polymers are sequentially layered onto the surface of the template.<sup>20</sup> For medical applications, the use of highly charged polymer materials may not be preferred since polyelectrolytes have known biological activities, such as anti- or procoagulation and protein binding.<sup>21–23</sup> Polycations often demonstrate the added problem of toxicity.<sup>24</sup> One advantage of this method is that a capsule shell can be formed from completely hydrophilic materials.

As an alternative, polymerization of a shell onto a core template may be utilized to form nanometer scale capsules. Interfacial polymerization of emulsions, often used to create microcapsules,<sup>25</sup> has not been developed to the same extent to create nanocapsules.<sup>26</sup> As a result, nanocapsules formed via polymerization have been primarily fabricated using colloids as templates. A variety of materials have been fabricated as nanoparticles exhibiting colloidal stability, thus providing a library of core templates from which to choose. This flexibility in material selection facilitates the identification of core templates that are stable during shell formation but may be subsequently removed.

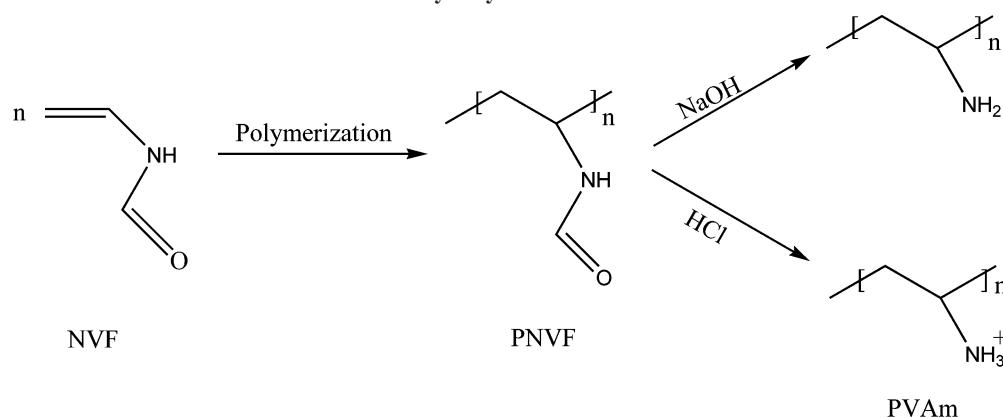
Multiple polymers have been reported for use as capsule shell forming materials. Historically, acrylates have received wide use. For this study, poly(*N*-vinylformamide) (PNVF) has been chosen due to the broad industrial use of polyvinyls and the ready reduction of this polymer to polyvinylamine (PVAm). PVAm has stable primary amine functionality along its backbone and may be partially or fully hydrolyzed to impart a low- or high-density polycation, respectively. This polymer has been employed in industrial applications such as inkjet printing, adhesives, industrial coatings, ion exchange resins (for separation-purification purposes), oil field and mining, and textiles. The high reactivity of amine groups provides important active sites for cross-linking and/or derivatization. Recently, PVAm has been used as a macromolecular carrier for the development of new detection reagents. For example, polyvinylamine–streptavidin conjugates labeled with a europium chelate were

\* To whom correspondence should be addressed: Ph (785) 864-1455, Fax (785) 864-1454, e-mail berkland@ku.edu.

<sup>†</sup> Department of Pharmaceutical Chemistry.

<sup>‡</sup> Department of Chemical and Petroleum Engineering.

Scheme 1. Hydrolysis of PNVF to PVAm



used in combination with biotinylated reagents (e.g., antibodies, DNA probes) for the development of highly sensitive solid-phase, time-resolved, fluorescence-based assays.<sup>27</sup> In addition, PVAm has been demonstrated as an effective gene delivery vector because of its ability to condense DNA, the complex exhibiting high stability and high gene expression in cells.<sup>28</sup>

We report the synthesis and characterization of pH-sensitive cationic polyvinylamine micro- and nanocapsules that are able to degrade more quickly at reduced pH. This effort builds upon the work of Frechet et al. regarding the use of hydrophilic polymers that degrade via acid-sensitive cross-linkers.<sup>29</sup> PVAm is a linear polycation, made by hydrolysis of PNVF using an aqueous solution of either HCl or NaOH (Scheme 1). The precursor polymer, PNVF, is obtained by free-radical polymerization of *N*-vinylformamide (NVF). In this study, a PNVF shell was formed on silica nanoparticles by cross-linking PNVF using a novel cross-linker, 2-bis[2,2'-di(*N*-vinylformamido)-ethoxy]propane (BDEP),<sup>30</sup> which contains an acid-labile ketal. PVAm nanocapsules were obtained by etching silica particles in NaOH under sonication followed by hydrolysis of PNVF through extended exposure to the NaOH aqueous solution (Figure 1). The size and shell thickness of capsules were easily adjusted by controlling the size of the silica template and the reaction time, respectively. The resulting nanocapsules demonstrated high stability at neutral pH (pH 7.4;  $t_{1/2} > 3$  days) compared to rapid dissolution observed at lower pH (pH 4;  $t_{1/2} = 42$  min). A high degree of swelling occurred in the PVAm capsules as pH decreased, which correlated with the relative charge (zeta potential) of PVAm nanocapsules. The methods

reported here provide a unique approach to generate micro- and nanocapsules with multiple desirable properties including size control, pH responsiveness, hydrolytic degradability, and surface functionality.

### Experimental Section

**Materials.** *N*-Vinylformamide (NVF; Aldrich) was distilled under vacuum and stored at  $-18^\circ\text{C}$  prior to use. The initiator, 1,1'-azobis(isobutyronitrile) (AIBN; Aldrich), was recrystallized from ethanol. All other materials were used without further purification including 1-octanol (Fischer Scientific), tetraethoxysilane (TEOS; Aldrich), 3-methacryloxypropyltrimethoxysilane (MPS; Aldrich), potassium *tert*-butoxide (Aldrich), 2-bromoethyl ether (tech, 90%; Aldrich), anhydrous tetrahydrofuran (THF; Aldrich), and poly(vinylpyrrolidone) (PVP,  $M_w = 360\,000$ ; Sigma). The pure water used was obtained from a Barnstead NANOpure water purifier. Silica particles were prepared as described previously.<sup>31</sup> MPS-coated silica particles as seeds were prepared as described previously.<sup>32</sup> 2,2-Dibromoethoxypropane was also prepared according to a previous report.<sup>33</sup> 2-Bis[2,2'-di(*N*-vinylformamido)-ethoxy]propane (BDEP) was prepared according to our previous report.<sup>30</sup>

**Preparation of PNVF Shell/Silica Particle Core Composite Nanoparticles.**<sup>30</sup> Briefly, to a suspension of MPS-modified silica particles (0.5 g) in ethanol (40 mL) was charged NVF (1.25 g), cross-linker (BDEP; 0.66 g), PVP (0.75 g), and AIBN (0.033 g) under stirring. After removing oxygen by bubbling with nitrogen for 15 min, the suspension was heated to  $70^\circ\text{C}$  and maintained at that temperature for 60 min. The composite particles were purified by centrifugation/dispersion for five cycles using ethanol.

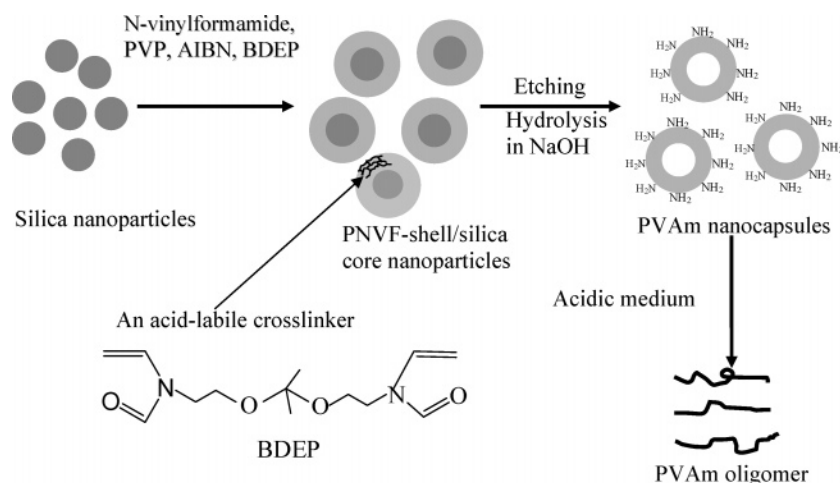


**Figure 1.** Schematic representation of the process for the preparation of PVAm capsules. PVP = poly(vinylpyrrolidone), AIBN = azobis(isobutyronitrile).

**Preparation of PNVF and Polyvinylamine (PVAm) Nanocapsules.** PNVF capsules were fabricated by etching silica in 1 M NaOH aqueous solution under sonication at room temperature. PVAm capsules were produced by subsequently hydrolyzing the shell polymer. Typically, PNVF shell/silica core composite particles (0.4 g) were dispersed into 1 M NaOH (40 mL) and sonicated at room temperature in a sonicating tank for 60 min. The capsules obtained were purified by dialysis (MW cutoff, 100 kDa) against water at pH 9.0 for 24 h.

**Determination of Formamide Conversion of Hydrolyzed PNVF Nanogel Capsules.** Formamide molar conversion of hydrolyzed PNVF capsules was determined by  $^1\text{H}$  NMR. Hydrolyzed PNVF capsules were dissolved in pH 5 acetic acid buffer, and then the solution was dialyzed in dialysis tubing ( $M_w$  cutoff, 2.0 kDa) against nanopure water 3 days. Dry polymer was recovered after freeze-drying. The NMR spectrum of hydrolyzed NVF in  $\text{D}_2\text{O}$  was recorded. The chemical shift of the aldehyde proton on formamide groups and  $-\text{CH}_2-$  are at 7.4–8.2 and 1.2–2.4 ppm, respectively. The molar conversion of formamide groups into amine groups after hydrolysis can be calculated by the equation as follows:

$$\text{formamide conversion} = 1 - 2 \times \frac{\text{aldehyde proton peak area}}{\text{CH}_2 \text{ peak area}}$$

We found that silica etching in 1 M NaOH resulted in the production of PNVF capsules that were  $30 \pm 5\%$  hydrolyzed. Further hydrolysis of the PNVF shell in 1 M NaOH at  $80^\circ\text{C}$  for 12 h produced PVAm capsules ( $100 \pm 5\%$  hydrolyzed) (see Figure 1 in Supporting Information).

**Conjugation of PVAm Capsules with FITC.** PVAm capsules (100 mg) were dispersed in sodium bicarbonate buffer at pH 9 (5 mL). Fluoroisothiocyanate (FITC; 11.07 mg) was dissolved in dry DMSO (5 mL), added to the PVAm capsule dispersion, and stirred overnight at room temperature. FITC-conjugated PVAm capsules were purified by centrifugation and dispersion in water at pH 9.0 for three cycles.

**Characterization of Materials and Nanocapsules.** IR spectra were recorded on a MB-104 FT-IR spectrometer (ABB Bomen Inc.). A Bruker AMX 500 spectrometer was used to record the NMR spectra of PNVF, hydrolyzed PNVF, and PVAm using  $\text{D}_2\text{O}$  as a solvent and tetramethylsilane as an internal standard. Particle sizes and size distributions of particles or capsules were determined at a  $90^\circ$  scattering angle by a Brookhaven BI-MAS. Zeta potential measurements were performed using a 1 mM KCl solution, the pH values of which were adjusted by addition of sodium hydroxide and hydrochloric acid between pH 6 and 12.

Dissolution kinetics of capsules at various pH was determined by using an 8453 UV/vis spectrophotometer (Agilent Technologies). About 10 mg of capsules was placed into a cuvette containing 3 mL of buffer solution at a given pH. The absorbance was measured at a fixed wavelength of 480 nm at  $25^\circ\text{C}$  at preselected time intervals. The pH of a suspension of PVAm capsules was monitored by an XL15 pH meter (Accument, Fisher Scientific) with a pH electrode (Thermo Electron Corp.).

TEM images of particles and capsules were obtained using a JEOL 1200 EXII transmission electron microscope operating at an accelerating voltage of 80 kV. Total internal reflectance illuminator microscopy images (TIRFM) of FITC-labeled polyvinylamine capsules were obtained by a fluorescence microscope (Olympus IX71) equipped with a total internal reflectance illuminator. The particles were excited with the 514 nm line of a Coherent Innova 70 Spectrum Kr/Ar laser and images collected with a Q imaging Retiga 1300 CCD.

The molecular weight and number of PNVF recovered after capsule degradation were determined by size exclusion chromatography (VE-2001; Viscotek) equipped with a Viscotek 270 dual detector and Viscotek VE3580 RI detector using a GMPWxl column (column size: 78 mm (i.d.)  $\times$  300 mm (L)). An aqueous mobile phase was used consisting of 0.1 M  $\text{NaNO}_3$  and 0.01%  $\text{NaN}_3$  at a flow rate of 1.0 mL/min at  $35^\circ\text{C}$ .

## Results

**Synthesis of PNVF and PVAm Capsules.** The procedure for the preparation of PNVF and PVAm capsules involved two steps (Figure 1). The first step requires coating silica particles with PNVF cross-linked by BDEP. Silica particles were chosen as templates because monodisperse silica particles can be readily synthesized by the Stöber method,<sup>12</sup> and silica can be easily etched by either in hydrofluoric acid<sup>39</sup> or concentrated NaOH. A series of PNVF shell/silica core composite particles were synthesized under the same polymerization conditions using silica particles ranging from 83 to 800 nm in diameter (Figure 2). A very thin PNVF shell ( $17 \pm 1.0$  nm) was detectable on the surface of the largest silica particles while relatively thicker shells ( $23 \pm 2.0$  nm) are evident on the smallest silica particles. The shell thickness of PNVF composite particles was readily controlled by controlling the polymerization time (Figure 3). PNVF shell thickness increased with polymerization time due to the increase in monomer conversion with time and curtailed as monomer was consumed. The PNVF shell/silica core composites with various sizes were easily dispersed in water, ethanol, and *tert*-butanol. In order to obtain PNVF-coated silica composites and avoid production of possible solid PNVF particles, it is important to maintain the polymerization temperature lower than  $70^\circ\text{C}$  and polymerization time less than 4 h. Solid PNVF particles at higher temperature and extended polymerization were observed, which is probably ascribed to the high reactivity of NVF and transfer of PNVF chain free radicals to PVP in the solution (NVF:  $C_m = 9.37 \times 10^4$  at  $60^\circ\text{C}$ ),<sup>34</sup> which produces new particle nuclei leading to the formation of PNVF particles.<sup>35</sup>

In the second step, the silica is etched and PNVF capsules may be hydrolyzed to a controlled degree. The removal of silica and extent of hydrolysis were controlled by the molarity of NaOH used and/or the exposure time of the composites to this milieu. Hydrofluoric acid is typically used to etch silica hybrid particles because it can easily dissolve  $\text{SiO}_2$ . On the contrary, hydrofluoric acid (HF) was not utilized in this research to produce PVAm capsules containing the acid-labile cross-linker because HF also breaks cross-linking points during extended periods of etching. NaOH was employed as an alternative etchant since it can also easily dissolve silica particles with the aid of sonication. The concentration of NaOH required is directly dependent on the amount of silica particles to be etched. We successfully fabricated acid-labile PVAm capsules by first etching silica particles in NaOH under sonication at room temperature followed by PNVF hydrolysis in NaOH at  $80^\circ\text{C}$ . One of the advantages of using this method is that we can control the conversion of amine groups of capsules by simply controlling hydrolysis time.<sup>36</sup> FTIR spectra verified each step of the fabrication process: PNVF shell/silica core composites cross-linked by BDEP, PNVF capsules after silica etched in 1 M NaOH at room temperature for 60 min and the resulting PVAm capsules after hydrolysis in 1 M NaOH aqueous solution at  $80^\circ\text{C}$  for 24 h, respectively (Figure 4). Compared to the peaks in the PNVF shell/silica core composites (Figure 4A), the peaks at  $1096\text{ cm}^{-1}$  (Si–O–Si asymmetric stretching) and  $811\text{ cm}^{-1}$  (Si–O bending) disappeared in the PNVF capsules (Figure 4B), which suggests that the silica particle templates were effectively removed by etching in 1 M NaOH at room temperature for 60 min. The peak at  $1666\text{ cm}^{-1}$  in spectra A and B is a characteristic peak of formamide groups in PNVF, which indicates that PNVF composites and capsules were produced, respectively. We suspected that the etching process may hydrolyze some of the formamide side groups along the



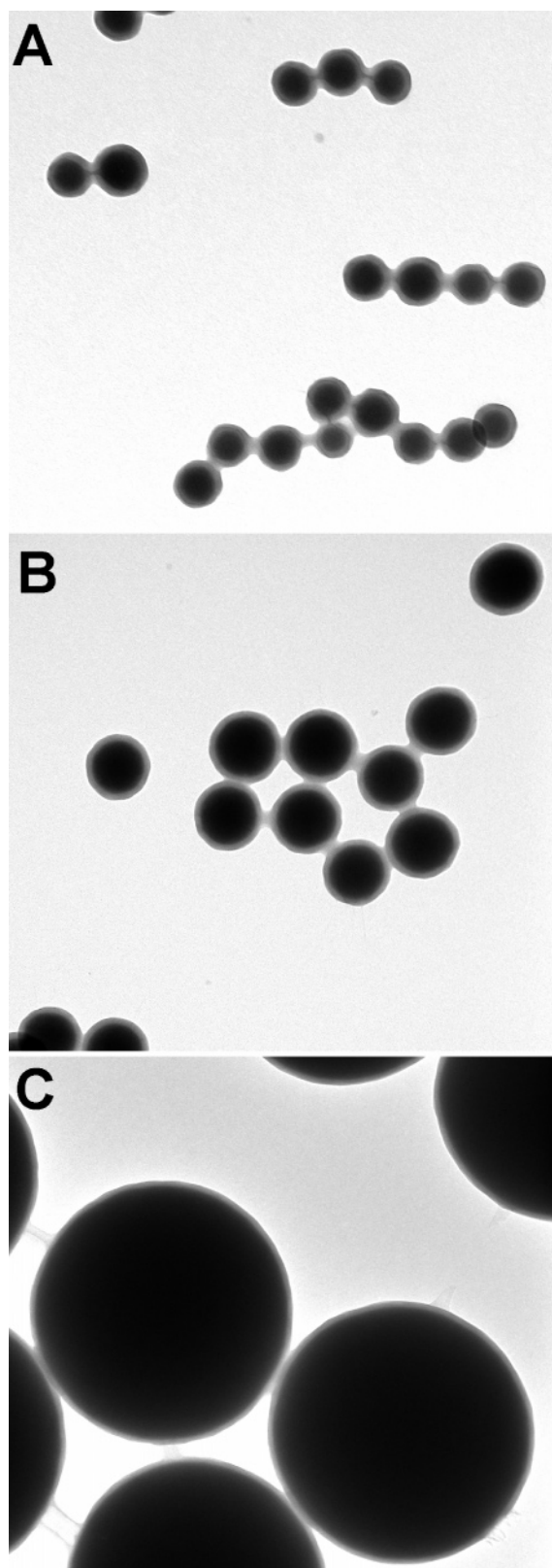


**Figure 2.** Fabrication of PNVF shell/silica core composite particles using different size silica templates prepared in ethanol in the presence of PVP as a stabilizer at 70 °C: (A) silica particle:  $83 \pm 5.3$  nm; PNVF shell:  $23 \pm 2.0$  nm; (B) silica particle:  $192 \pm 10.2$  nm; PNVF shell:  $19 \pm 1.0$  nm; (C) silica particle:  $800 \pm 5.1$  nm; PNVF shell:  $17 \pm 1.0$  nm.

polyvinyl backbone. Although the FTIR spectrum did not distinctly show characteristic peaks of amine side groups on the PNVF capsules,  $^1\text{H}$  NMR revealed that  $\sim 30\%$  of formamide groups were converted into amine groups ( $^1\text{H}$  NMR data are

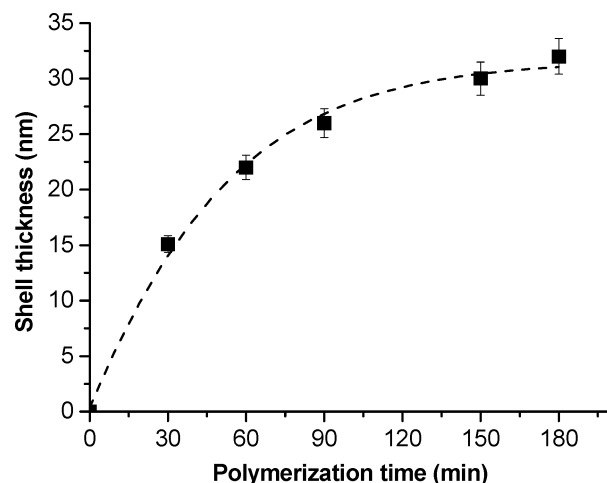


**Figure 3.** PNVF shell thickness as a function of polymerization time using the prescribed methods on 165 nm silica particles at 70 °C.

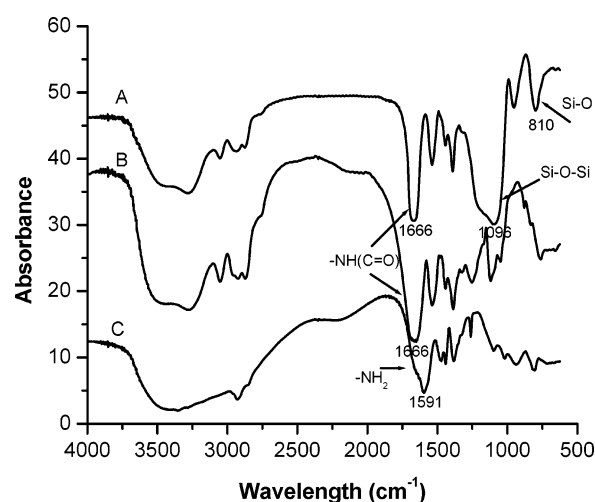


**Figure 4.** IR spectra verified chemical signatures of (A) PNVF shell/silica core composite particles, (B) PNVF capsules after silica etching ( $\sim 30\%$  conversion of formamide to amine), and (C) PVAm capsules.

given in Figure 1B in the Supporting Information). The disappearance of the peak at  $1666\text{ cm}^{-1}$  and appearance of a characteristic peak of  $\text{NH}_2$  at  $1591\text{ cm}^{-1}$  after extended treatment of PNVF capsules with 1 M NaOH proved that PVAm capsules were produced under the given hydrolysis conditions (formamide conversion  $\sim 100\%$ ) ( $^1\text{H}$  NMR data are shown in Figure 1C in the Supporting Information).

TEM images provided supporting evidence of the capsule fabrication process (Figure 5). Cross-linked PNVF shell/silica core composites, PNVF capsules after silica was etched out in 1 M NaOH at room temperature for 60 min, and PVAm capsules after hydrolysis in 1 M NaOH aqueous solution at 80 °C for 12 h were clearly depicted by TEM. The inner diameter of both PNVF and PVAm capsules became smaller than that of the corresponding silica particles used as templates due to the shrinkage of capsules upon evaporation of ethanol during TEM sample preparation. In solution at pH higher than 11.0, PNVF capsules exhibited a diameter close to the corresponding PNVF composites prior to silica etching. Uniform shell sizes and inner diameters of both PNVF and PVAm capsules are evident. The PVAm capsule shell ( $23 \pm 0.5$  nm) was significantly thicker than the corresponding PNVF capsule shell ( $19 \pm 1.0$  nm), even in the dried state. The core diameter was also decreased in PVAm capsules ( $57 \pm 3.9$  nm) as compared to PNVF capsules ( $68 \pm 7.3$  nm). We hypothesize that the highly charged PVAm

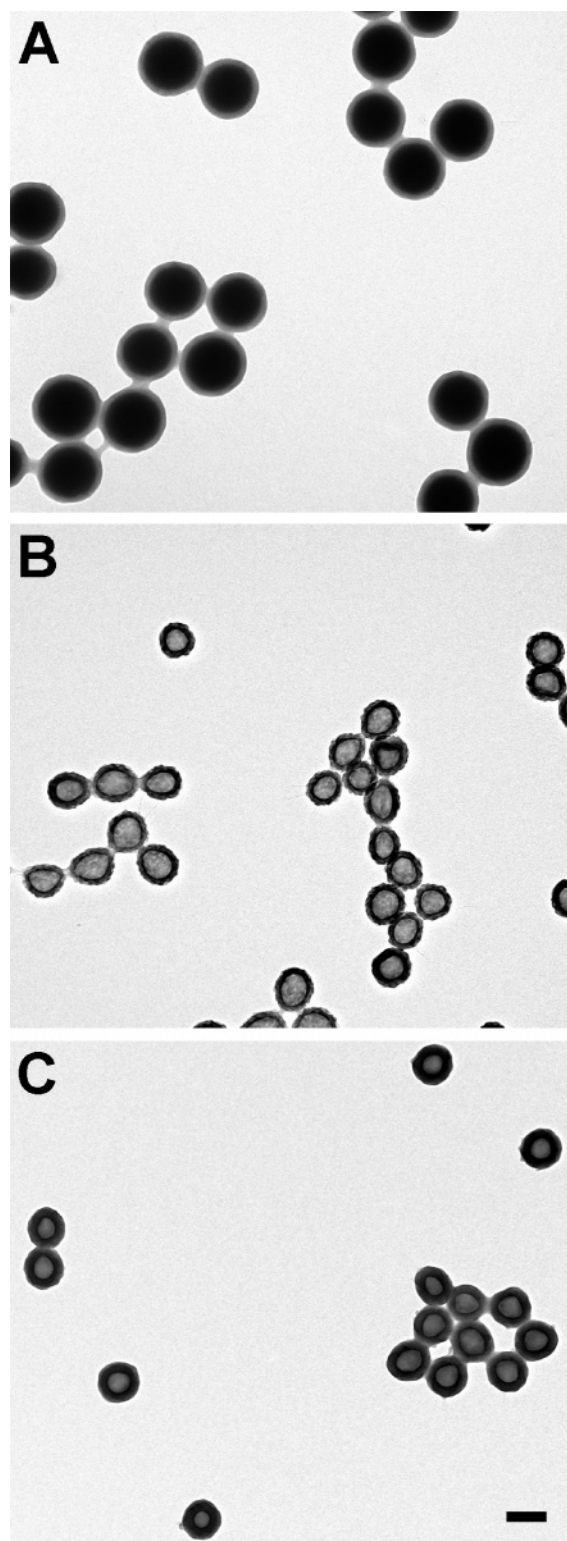


**Figure 5.** TEM images of the PVAm capsule fabrication process confirmed each step. (A) PNVF shell/silica core composite particles: PNVF shell thickness:  $18 \pm 1.0$  nm; core diameter:  $127 \pm 6.2$  nm. (B) PNVF capsules: PNVF shell thickness:  $19 \pm 1.0$  nm; core diameter:  $68 \pm 7.3$  nm. (C) PVAm capsules: PVAm shell thickness:  $23 \pm 0.5$  nm; core diameter:  $57 \pm 3.9$  nm. Scale bar = 100 nm.

produces swelling due to charge repulsion within the cross-linked polymer. This phenomenon is expanded upon below.

**Degradation of PVAm Capsules in Acidic Medium.** The degradation of PVAm capsules was determined as a function of pH using a turbidity assay, where the optical density of the suspension at 480 nm indicated the relative concentration of

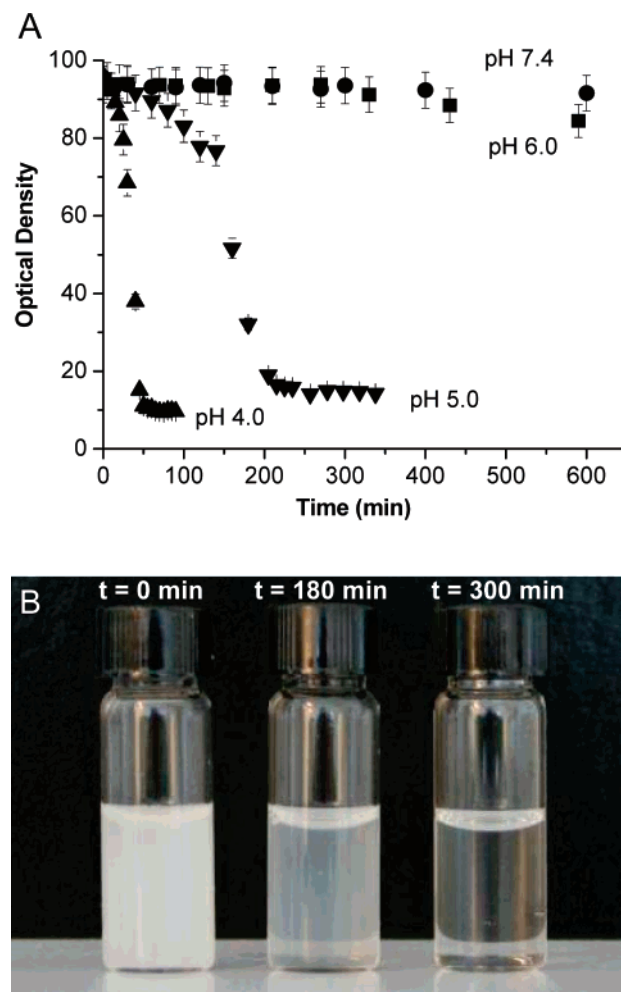


**Figure 6.** Degradation of PVAm capsules (average shell thickness is 18 nm and core diameter is 127 nm) over time strongly depended upon media pH as determined by (A) a turbidity measurement of PVAm capsules over time as a function of pH and confirmed by (B) visualization of the degradation of PVAm capsules into soluble PVAm in pH 5 buffer over time.

**Table 1. Half-Life of Degradation of PVAm Capsules as a Function of pH**

pH	4.0	5.0	6.0	7.4
half-life ( $t_{1/2}$ )	42 min	160 min	~24 h	>3 days

PVAm capsules in solution (Figure 6A). We chose concentrations of capsules in suspension so that the initial optical density of the particle suspension was close to 100%. Degradation of PVAm capsules occurred rapidly at acidic pH. Conversely, the slight decrease in optical density of the suspension at higher pH values (6.0 and 7.4) indicated that the particles degraded much more slowly. The relative half-life of PVAm capsules was estimated from the midpoint of the optical density curve (Table 1).

The degradation of PVAm capsules in acidic buffer was ascribed to the breakdown of ketal-containing cross-links in the PVAm shell. The existence of BDEP residue on the PVAm shell after ketal linkage breakdown was confirmed by  $^1\text{H}$  NMR measurement. Compared to proton NMR spectrum of PVAm, a new proton peak at 3.60 ppm was ascribed to the protons ( $-\text{CH}_2\text{CH}_2\text{OH}$ ) of the BDEP residue (Figure 7). The degradation kinetics of PVAm capsules was strongly dependent on the pH of the surrounding milieu because the hydrolysis rate of ketals under acid catalyst is proportional to the hydronium ion concentration in solution.<sup>37</sup> For example, Frechet et al. dem-

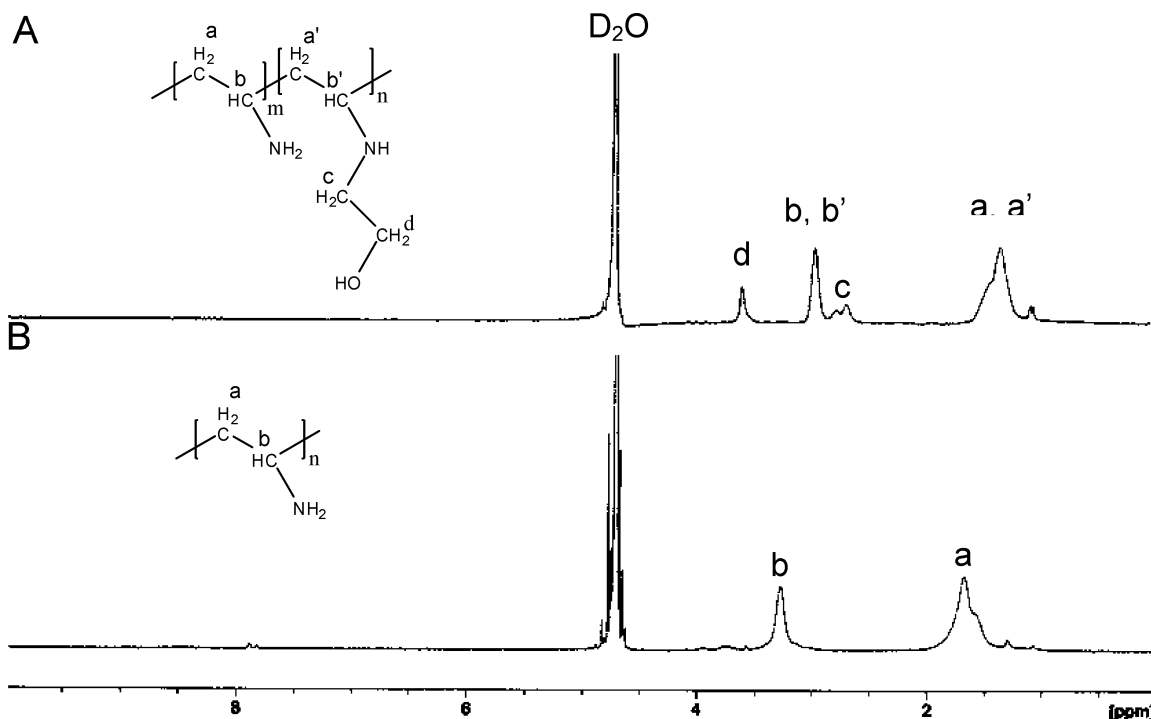


**Figure 7.** Comparison of <sup>1</sup>H NMR spectrum of PVAm obtained by degradation of BDEP-cross-linked PVAm capsules (A) with PVAm (B).

onstrated that ketals were hydrolyzed ~250 times faster at pH 5.0 than at pH of 7.4 for the case of solid microgels.<sup>38</sup> The degradation of PVAm capsules was also confirmed by visually tracking solution opacity at pH 5 over 5 h (Figure 6B). The initially opaque PVAm capsule suspension at pH 5 turned completely clear within 300 min, which indicated that all particles were degraded and that PNVF oligomers were dissolved in the medium.

Multiple factors directly influenced the degradation kinetics of the two types of polyvinyl capsules. Obviously, the extent of cross-linking may be manipulated to adjust the degradation rate of capsules. For example, doubling the molar content of cross-linker from 6.56% to 13.2% in PVAm capsules resulted in a ~3-fold increase in capsule half-life at pH 5.0 and produced more gradual degradation kinetics (Figure 8A). Interestingly, the presence of amine side groups also dramatically affected the degradation of capsules. <sup>1</sup>H NMR was used to confirm that ~30% of the formamide side groups were converted to amine side groups during the etching of silica particle templates to form PNVF capsules (see Figure 1B in the Supporting Information). At pH 4.7, PNVF capsules (~30% amine conversion) exhibited a ~2.5 fold shorter half-life than PVAm capsules that contained ~100% amine conversion (Figure 8B). We hypothesize that the presence of the amine side groups may have a localized buffering effect in that hydronium ions necessary to break the ketal cross-linker associated with amine groups in the capsule matrix. Therefore, increasing the percentage of hydrolyzed formamide side groups may have provided more sites for hydronium ion capture and extended the degradation half-life of capsules. This hypothesis was further supported by observing the effect of PVAm capsule concentration on the degradation half-life (Figure 8C). Increasing the concentration of PVAm capsules (~100% hydrolyzed) increased the pH of the dissolution media and linearly increased the degradation half-life (Figure 8D). For the PVAm capsule concentrations studied, the original solution was buffered at pH 4; however, the reduction in cross-linker degradation as capsule concentration increased may again be attributed to the ability of amine side

groups to occupy hydronium ions (buffering effect). Finally, the localized buffering effect may be reflected in the sigmoidal degradation kinetics for all formulations, which do not follow the linear ketal degradation observed in previous reports.<sup>29</sup>

In order to obtain the molecular weight of products after capsule degradation, we dissolved PNVF shell/silica core composites cross-linked with BDEP in 10% HF. The degraded PNVF was obtained after dialysis of the PNVF solution against water for 24 h to remove etched silica and retain PNVF oligomers. FTIR and NMR spectra confirmed that PNVF did not undergo hydrolysis during the dissolution of the particles in 10% HF (<sup>1</sup>H NMR data are given in Figure 2B in the Supporting Information). The molecular weight of the recovered PNVF was 14 800 Da, and the molecular weight distribution was 1.45.

**Comparison of Charge and Swelling of PNVF and PVAm Capsules.** Zeta potential measurements were employed to evaluate the surface charge of capsules (Figure 9). For this study, larger capsules were used, which allowed confirmation of the capsule size by total internal fluorescence illuminator microscopy (TIRIF) as well as detection of zeta potential and accurate determination of capsule size by QELS, all with respect to pH. PVAm capsules possessed a positive zeta potential below pH 10.7. The zeta potential increased with decreasing pH, indicating the presence of protonated amine groups as expected. At pH 10.7, the capsules have a zeta potential of ~0 mV because the pK<sub>a</sub> of PVAm is ~10.<sup>39</sup> Examining the PNVF capsules postetching but prior conversion to PVAm produced similar trends; however, the magnitude of the change in zeta potential as a function of pH was dampened for the PNVF capsules due to the significant reduction of amine side groups on the capsules (~30% amine conversion). The observation of comparable, although dampened, zeta potential trends was again attributed to the charged state of the amine side groups on PNVF capsules.

The diameter of PVAm capsules also exhibited a corresponding pH dependency. PVAm capsules drastically decreased in diameter with increasing pH (~1.7-fold diameter change over 4 pH units). The pH dependence of PVAm capsule size



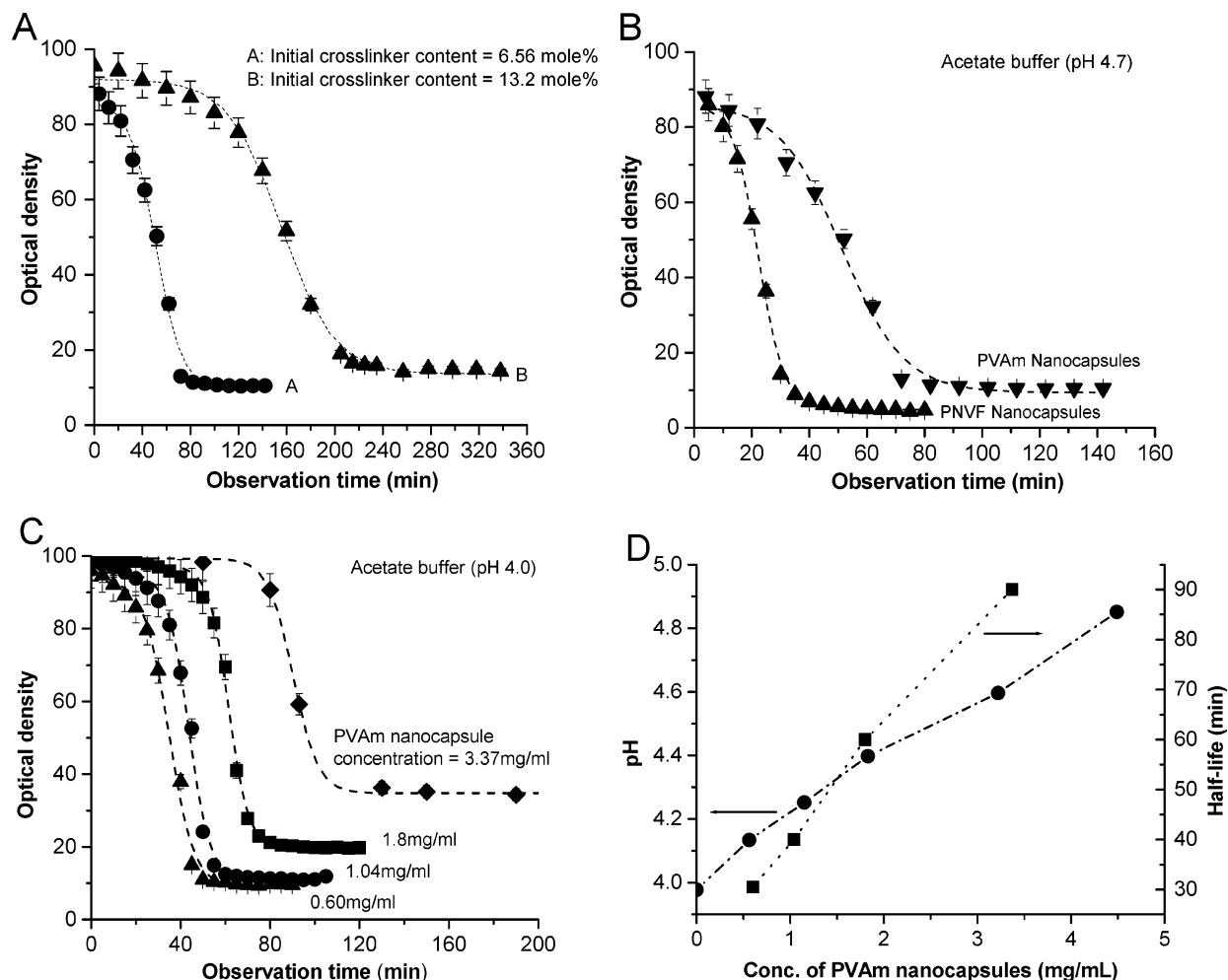


**Figure 8.** Optical density of capsule suspensions was tracked over time to deduce a variety of parameters affecting the degradation rate of the cross-linked capsules. (A) Degradation rate of PVAm capsules as a function of cross-linking density. (B) Degradation rate as a function of capsule hydrolysis: PVAm capsules ~100% hydrolyzed, PNVF capsules ~30% hydrolyzed. (C) Degradation rate as a function of PVAm capsule concentration. (D) pH value of medium as a function of increasing PVAm capsule concentration.

correlated extremely well to changes in PVAm protonation (Figure 9). A similar correlation between zeta potential and capsule size was also observed for PNVF capsules (~30% hydrolyzed).<sup>6,40</sup> Total internal fluorescence illuminator micrographs (TIFIM) provided visual evidence that PVAm capsules (in this case, microcapsules) are hollow and have a larger size at pH 6.8 than at pH 11 (Figure 10).

For comparison, we also fabricated PNVF shell/silica core composite particles with a PNVF shell cross-linked by a nondegradable cross-linker, 2-(*N*-vinylformamide)ethyl ether, in which the ketal was replaced by an oxygen atom (see Figure 3 in the Supporting Information). Here, we employed HF (10%) instead of concentrated NaOH to etch silica to avoid formamide group hydrolysis during the etching process because HF can dissolve silica readily.<sup>39</sup> As expected, these PNVF capsules possessed negligible sensitivity to pH, maintaining a near constant zeta potential (~0 mV) and size (Figure 9).

The change in size of PVAm capsules in response to pH can be ascribed to contributions from the free energies associated with mixing of polymer with solvent ( $\Delta G_M$ ), with network elasticity ( $\Delta G_E$ ), and with ionic contribution ( $\Delta G_{ion}$ ), which strongly depends on ionic strength and the nature of the ions.<sup>41</sup> The general expression is given as an expression of the total free energy in the system ( $\Delta G$ ):

$$\Delta G = \Delta G_M + \Delta G_E + \Delta G_{ion}$$

PVAm capsules contain pendent amine groups that are cationic or neutral in nature, determined by their  $pK_a$  and solution pH. When PVAm capsules are placed in medium of pH below its  $pK_a$ , the protonated amine groups are ionized and neutralized by counterions in solution resulting in an osmotic pressure, which swells the particle against its restoring elastic constant.<sup>42</sup> Therefore, a decreased pH increases the degree of protonation and corresponding counterion content of PVAm capsules, causing the particle to further swell. On the contrary, a further increase in pH beyond the  $pK_a$  of the amine side chains was not possible to explore since colloidal stability of capsules was lost when passing pH ~11.

## Conclusions

As nanomaterials begin to enter the industrial mainstream, enhanced performance will be required. Performance may be gained by precisely defining the physical and chemical properties of these materials. By using essentially monodispersed silica micro- and nanoparticles as sacrificial templates, polyvinyl micro- and nanocapsules may be synthesized by the method described with excellent control over the core diameter. In addition, the shell thickness of capsules may be precisely modulated by controlling the monomer concentration, reaction rate, and duration of free radical polymerization. The polymerization of NVF in the presence of a novel, acid-labile cross-linker maintained capsule integrity during silica etching at high

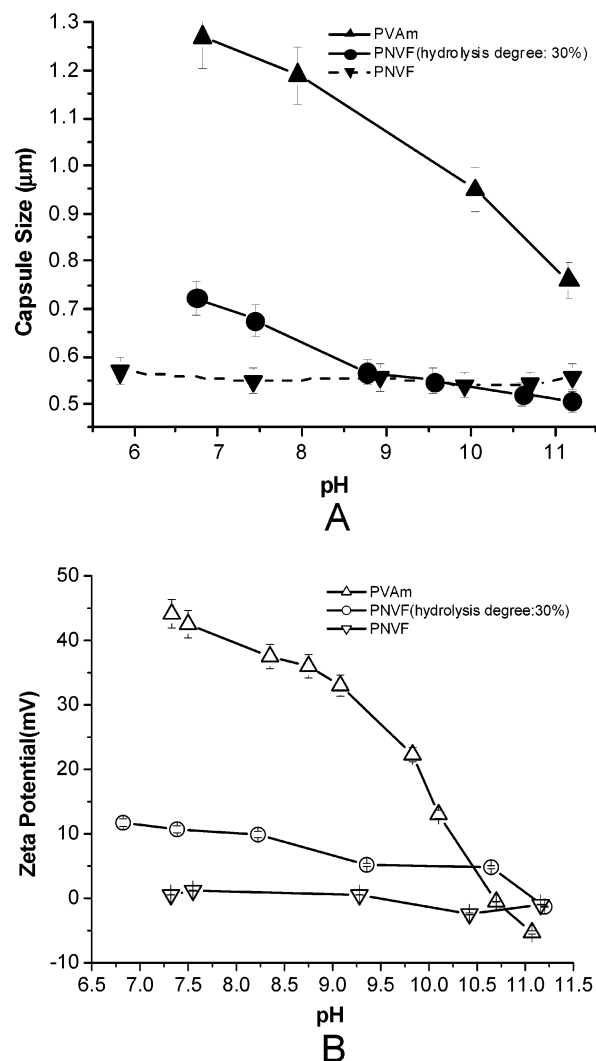


**Figure 9.** Size (A) and zeta potential (B) of PVAm capsules decreased as pH increased. The zeta potential and size of PNVF capsules (~30% hydrolyzed) showed similar trends at a lower magnitude, but PNVF unhydrolyzed capsules exhibited no sensitivity to pH.

pH and allowed us to infuse pH responsiveness into polyvinyl capsules. The resulting PNVF capsules possessed colloidal stability in a variety of media such as water, ethanol, and toluene.

PNVF capsules were further processed by hydrolysis of the formamide side group to generate PVAm capsules as confirmed by FTIR and NMR. Both types of capsules demonstrated increasingly rapid degradation as pH was decreased. PVAm capsules also showed increased swelling as pH decreased that depended on the degree of amine conversion. The magnitude of swelling correlated well with the increase in zeta potential of the suspension as pH was lowered. Presumably, the increased number (amine conversion) and/or charging (pH) of protonated amine groups resulted in a stretching of the cross-linked polymer network. Taken collectively, acid-labile PVAm capsules offer a synthetic approach for adding performance to these nanomaterials. Future work will explore loading therapeutics or imaging agents into PVAm capsules by selective diffusion into the core or utilizing core templates preloaded with active ingredient.

**Acknowledgment.** We are grateful to the Cystic Fibrosis Foundation for supporting a portion of this research as well as support for our lab from the Juvenile Diabetes Research Foundation, the American Heart Association, the Department

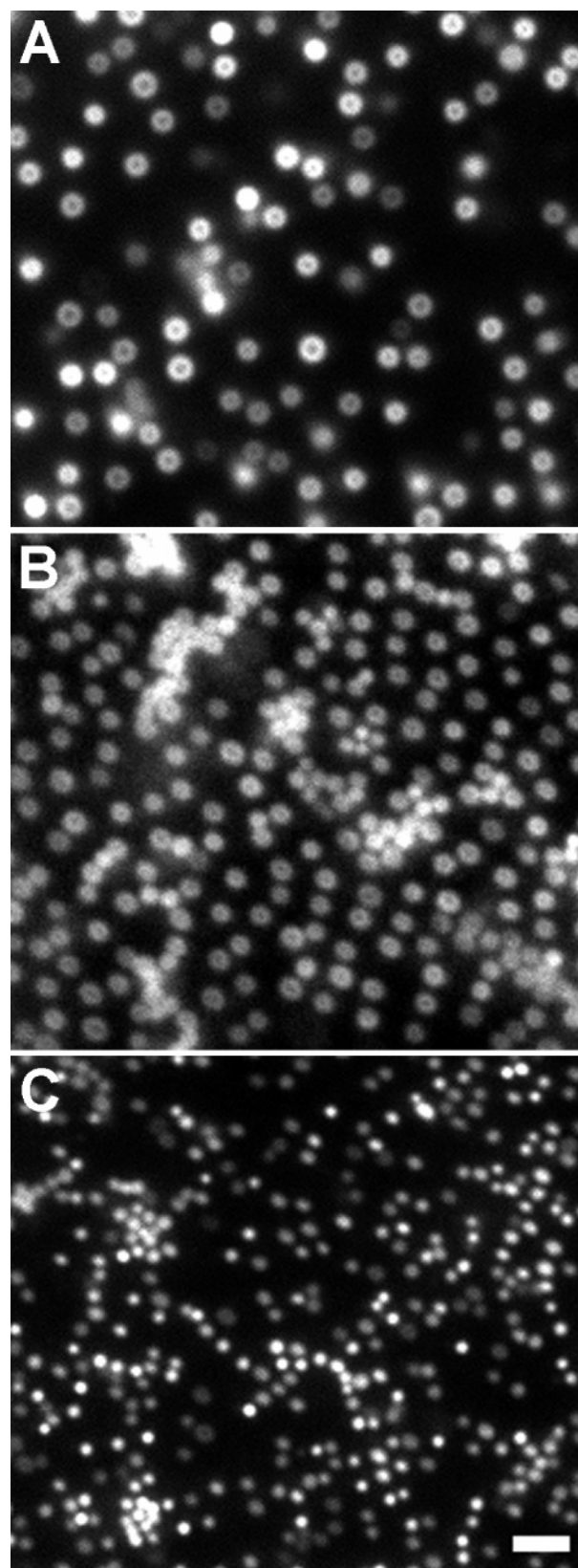


**Figure 10.** Total internal fluorescence illuminator micrographs of PVAm capsules at (A) pH 6.8, (B) pH 7.4, and (C) pH 11. Scale bar = 2 μm.

of Defense, and the NIH (P20 RR016443 and P20 RR015563). We also thank Prof. C. Russ Middaugh for the use of laboratory equipment, Prof. Robert Dunn for the use of TIFIM, and The Microscopy Lab for imaging assistance.



**Supporting Information Available:**  $^1\text{H}$  NMR spectra of PNVF, PVAM with BDEP residue, and PNVF with BDEP residue (Figures 1 and 2) and structure of 2-(*N*-vinylformamide)ethyl ether (Figure 3). This material is available free of charge via the Internet at <http://pubs.acs.org>.

## References and Notes

- (1) Mathiowitz, E. *Encyclopedia of Controlled Drug Delivery*; John Wiley & Sons: New York, 1999; Vols. 1 and 2.
- (2) Zhu, H. G.; McShane, M. J. Loading of hydrophobic materials into polymer particles: Implications for fluorescent nanosensors and drug delivery. *J. Am. Chem. Soc.* **2005**, *127*, 13448–13449.
- (3) Muraoka, M.; Hu, Z. P.; Shimokawa, T.; Sekino, S.; Kurogoshi, R.; Kuboi, Y.; Yoshikawa, Y.; Takada, K. Evaluation of intestinal pressure-controlled colon delivery capsule containing caffeine as a model drug in human volunteers. *J. Controlled Release* **1998**, *52*, 119–129.
- (4) Blackmer, G. L.; Reynolds, R. H. *J. Agric. Food Chem.* **1977**, *25*, 559–561.
- (5) Meier, W. Polymer nanocapsules. *Chem. Soc. Rev.* **2000**, *29*, 295–303.
- (6) Kozlovskaya, V.; Sukhishvili, S. A. Amphoteric hydrogel capsules: Multiple encapsulation and release routes. *Macromolecules* **2006**, *39*, 6191–6199.
- (7) Koide, A.; Kishimura, A.; Osada, K.; Jang, W. D.; Yamasaki, Y.; Kataoka, K. Semipermeable polymer vesicle (PICsome) self-assembled in aqueous medium from a pair of oppositely charged block copolymers: Physiologically stable micro-/nanocapsules of water-soluble macromolecules. *J. Am. Chem. Soc.* **2006**, *128*, 5988–5989.
- (8) Wong, M. S.; Cha, J. N.; Choi, K. S.; Deming, T. J.; Stucky, G. D. Assembly of nanoparticles into hollow spheres using block copolypeptides. *Nano Lett.* **2002**, *2*, 583–587.
- (9) Sukhorukov, G. B.; Donath, E.; Davis, S.; Lichtenfeld, H.; Caruso, F.; Popov, V. I.; Mohwald, H. Stepwise polyelectrolyte assembly on particle surfaces: a novel approach to colloid design. *Polym. Adv. Technol.* **1998**, *9*, 759–767.
- (10) Donath, E.; Sukhorukov, G. B.; Caruso, F.; Davis, S. A.; Mohwald, H. Novel hollow polymer shells by colloid-templated assembly of polyelectrolytes. *Angew. Chem., Int. Ed.* **1998**, *37*, 2202–2205.
- (11) Dahne, L.; Leporatti, S.; Donath, E.; Mohwald, H. Fabrication of micro reaction cages with tailored properties. *J. Am. Chem. Soc.* **2001**, *123*, 5431–5436.
- (12) Xu, X. L.; Asher, S. A. Synthesis and utilization of monodisperse hollow polymeric particles in photonic crystals. *J. Am. Chem. Soc.* **2004**, *126*, 7940–7945.
- (13) Tissot, I.; Novat, C.; Lefebvre, F.; Bourgeat-Lami, E. Hybrid latex particles coated with silica. *Macromolecules* **2001**, *34*, 5737–5739.
- (14) Fleming, M. S.; Mandal, T. K.; Walt, D. R. Nanosphere-microsphere assembly: Methods for core-shell materials preparation. *Chem. Mater.* **2001**, *13*, 2210–2216.
- (15) Discher, B. M.; Won, Y. Y.; Ege, D. S.; Lee, J. C.; Bates, F. S.; Discher, D. E.; Hammer, D. A. Polymersomes: tough vesicles made from diblock copolymers. *Science* **1999**, *284*, 1143–6.
- (16) Lee, J. C.; Bermudez, H.; Discher, B. M.; Sheehan, M. A.; Won, Y. Y.; Bates, F. S.; Discher, D. E. Preparation, stability, and in vitro performance of vesicles made with diblock copolymers. *Biotechnol. Bioeng.* **2001**, *73*, 135–45.
- (17) Ahmed, F.; Pakunlu, R. I.; Srinivas, G.; Brannan, A.; Bates, F.; Klein, M. L.; Minko, T.; Discher, D. E. Shrinkage of a rapidly growing tumor by drug-loaded polymersomes: pH-triggered release through copolymer degradation. *Mol. Pharmaceutics* **2006**, *3*, 340–50.
- (18) Photos, P. J.; Bacakova, L.; Discher, B.; Bates, F. S.; Discher, D. E. Polymer vesicles in vivo: correlations with PEG molecular weight. *J. Controlled Release* **2003**, *90*, 323–34.
- (19) Li, X.; Hu, Q.; Yue, L.; Shen, J. Synthesis of size-controlled acid-resistant hybrid calcium carbonate microparticles as templates for fabricating “micelles-enhanced” polyelectrolyte capsules by the LBL technique. *Chemistry* **2006**, *12*, 5770–8.
- (20) Khopade, A. J.; Arulsudar, N.; Khopade, S. A.; Knocke, R.; Hartmann, J.; Mohwald, H. From ultrathin capsules to bioaqueous vesicles. *Biomacromolecules* **2005**, *6*, 3433–9.
- (21) Greinacher, A. Heparin-induced thrombocytopenia: frequency and pathogenesis. *Pathophysiol Haemost Thromb* **2006**, *35*, 37–45.
- (22) Jones, L. S.; Yazzie, B.; Middaugh, C. R. Polyanions and the proteome. *Mol. Cell. Proteomics* **2004**, *3*, 746–69.
- (23) Kwon, H. J.; Kakugo, A.; Shikina, K.; Osada, Y.; Gong, J. P. Morphology of actin assemblies in response to polycation and salts. *Biomacromolecules* **2005**, *6*, 3005–9.
- (24) Forrest, M. L.; Koerber, J. T.; Pack, D. W. A degradable polyethyleneimine derivative with low toxicity for highly efficient gene delivery. *Bioconjugate Chem.* **2003**, *14*, 934–40.
- (25) Ma, G. H.; Su, Z. G.; Omi, S.; Sundberg, D.; Stubbs, J. Microencapsulation of oil with poly(styrene-*N,N*-dimethylaminoethyl methacrylate) by SPG emulsification technique: effects of conversion and composition of oil phase. *J. Colloid Interface Sci.* **2003**, *266*, 282–94.
- (26) Beduneau, A.; Saulnier, P.; Anton, N.; Hindre, F.; Passirani, C.; Rajerison, H.; Noiret, N.; Benoit, J. P. Pegylated nanocapsules produced by an organic solvent-free method: Evaluation of their stealth properties. *Pharm. Res.* **2006**, *23*, 2190–9.
- (27) Scorilas, A.; Diamandis, E. P. Polyvinylamine-streptavidin complexes labeled with a europium chelator: A universal detection reagent for solid-phase time resolved fluorometric applications. *Clin. Biochem.* **2000**, *33*, 345–350.
- (28) Wolfert, M. A.; Dash, P. R.; Nazarova, O.; Oupicky, D.; Seymour, L. W.; Smart, S.; Strohalm, J.; Ulbrich, K. Polyelectrolyte vectors for gene delivery: Influence of cationic polymer on biophysical properties of complexes formed with DNA. *Bioconjugate Chem.* **1999**, *10*, 993–1004.
- (29) Murthy, N.; Xu, M.; Schuck, S.; Kunisawa, J.; Shastri, N.; Frechet, J. M. A macromolecular delivery vehicle for protein-based vaccines: acid-degradable protein-loaded microgels. *Proc. Natl. Acad. Sci. U.S.A.* **2003**, *100*, 4995–5000.
- (30) Berkland, C.; Shi, L. pH-Triggered Dispersion of Nanoparticle Clusters. *Adv. Mater.* **2006**, *18*, 2315–2319.
- (31) Stöber, W. F. A.; Bohn, E. Controlled Growth of Monodisperse Silica Spheres in the Micron Size Range. *J. Colloid Interface Sci.* **1968**, *26*, 62–69.
- (32) Bourgeat-Lami, E.; Lang, J. Encapsulation of inorganic particles by dispersion polymerization in polar media. 1. Silica nanoparticles encapsulated by polystyrene. *J. Colloid Interface Sci.* **1998**, *197*, 293–308.
- (33) Lorette, N. B.; Howard, W. L. Preparation of Ketals from 2,2-Dimethoxypropane. *J. Org. Chem.* **1960**, *25*, 521–525.
- (34) Gu, L.; Zhu, S.; Hrymak, A. N.; Pelton, R. H. Kinetics and modeling of free radical polymerization of *N*-vinylformamide. *Polymer* **2001**, *42*, 3077–3086.
- (35) Uyama, H.; Kato, H.; Kobayashi, S. Preparation of Monodisperse Poly-(*N*-Vinylformamide) Particles by Dispersion Polymerization in Methanol Solvent. *Chem. Lett.* **1993**, *2*, 261–262.
- (36) Gu, L.; Zhu, S.; Hrymak, A. N. Acidic and basic hydrolysis of poly-(*N*-vinylformamide). *J. Appl. Polym. Sci.* **2002**, *86*, 3412–3419.
- (37) Cordes, E. H.; Bull, H. G. Mechanism and catalysis for hydrolysis of acetals, ketals, and ortho esters. *Chem. Rev.* **1974**, *74*, 581–603.
- (38) Kwon, Y. J. S. S.; Goodwin, A. P.; Gillies, E. R.; Frechet, J. M. Directed antigen presentation using polymeric microparticulate carriers degradable at lysosomal pH for controlled immune responses. *Mol. Pharmaceutics* **2005**, *2*, 83–91.
- (39) Sumaru, K.; Matsuoka, H.; Yamaoka, H. Exact evaluation of characteristic protonation of poly(vinylamine) in aqueous solution. *J. Phys. Chem.* **1996**, *100*, 9000–9005.
- (40) Kudaibergenov, S. E.; Sigitov, V. B. Swelling, shrinking, deformation, and oscillation of polyampholyte gels based on vinyl 2-aminoethyl ether and sodium acrylate. *Langmuir* **1999**, *15*, 4230–4235.
- (41) Brannon-Peppas, L.; Peppas, N. A. Equilibrium Swelling Behavior of Ph-Sensitive Hydrogels. *Chem. Eng. Sci.* **1991**, *46*, 715–722.
- (42) Flory, P. J. *Principles of Polymer Chemistry*; Cornell University Press: Ithaca, NY, 1953; pp 432–594.

MA070443O